

RESEARCH ARTICLE

Maternal obesity alters offspring liver and skeletal muscle metabolism in early post-puberty despite maintaining a normal post-weaning dietary lifestyle

Isaac Ampong^{1,2} | Kip D. Zimmerman^{1,2} | Danu S. Perumalla^{1,2} |
 Katharyn E. Wallis^{1,2} | Ge Li^{1,2} | Hillary F. Huber³ | Cun Li⁴ |
 Peter W. Nathanielsz^{3,4} | Laura A. Cox^{1,2,3} | Michael Olivier^{1,2} 

¹Center for Precision Medicine, Wake Forest University School of Medicine, Winston-Salem, North Carolina, USA

²Department of Internal Medicine, Section on Molecular Medicine, Wake Forest University School of Medicine, Winston-Salem, North Carolina, USA

³Southwest National Primate Research Center, Texas Biomedical Research Institute, San Antonio, Texas, USA

⁴Center for Pregnancy & Newborn Research, University of Wyoming, Laramie, Wyoming, USA

Correspondence

Isaac Ampong and Michael Olivier, Center for Precision Medicine, Wake Forest University School of Medicine, Winston-Salem, NC, USA.

Email: iampong@wakehealth.edu and molivier@wakehealth.edu

Funding information

HHS | National Institutes of Health (NIH), Grant/Award Number: U19 AG057758

Abstract

Maternal obesity (MO) during pregnancy is linked to increased and premature risk of age-related metabolic diseases in the offspring. However, the underlying molecular mechanisms still remain not fully understood. Using a well-established nonhuman primate model of MO, we analyzed tissue biopsies and plasma samples obtained from post-pubertal offspring (3–6.5y) of MO mothers ($n = 19$) and from control animals born to mothers fed a standard diet (CON, $n = 13$). All offspring ate a healthy chow diet after weaning. Using untargeted gas chromatography-mass spectrometry metabolomics analysis, we quantified a total of 351 liver, 316 skeletal muscle, and 423 plasma metabolites. We identified 58 metabolites significantly altered in the liver and 46 in the skeletal muscle of MO offspring, with 8 metabolites shared between both tissues. Several metabolites were changed in opposite directions in males and females in both liver and skeletal muscle. Several tissue-specific and 4 shared metabolic pathways were identified from these dysregulated metabolites. Interestingly, none of the tissue-specific metabolic changes were reflected in plasma. Overall, our study describes characteristic metabolic perturbations in the liver and skeletal muscle in MO offspring, indicating that metabolic programming in utero persists postnatally, and revealing potential novel mechanisms that may contribute to age-related metabolic diseases later in life.

KEYWORDS

developmental programming, maternal obesity, metabolic disorders, metabolism, metabolomics

Abbreviations: CON, control; FC, fold change; FDR, false discovery rate; GC, gas chromatography; HFD, high fat and high energy diet; LC, liquid chromatography; LCMS, liquid chromatography mass spectrometry; MeOX, methoxyamine hydrochloride; MO, maternal obesity; MS, mass spectrometry; MSTFA, N-Methyl-N-trimethylsilyltrifluoroacetamide; MTBSTFA, N-(t-butyltrimethylsilyl)-N-methyltrifluoroacetamide; NHP, non-human primate; PCA, principal component analysis; sPLS-DA, sparse partial least squares discriminant analysis.

This is an open access article under the terms of the [Creative Commons Attribution-NonCommercial-NoDerivs](https://creativecommons.org/licenses/by-nc-nd/4.0/) License, which permits use and distribution in any medium, provided the original work is properly cited, the use is non-commercial and no modifications or adaptations are made.

© 2022 The Authors. *The FASEB Journal* published by Wiley Periodicals LLC on behalf of Federation of American Societies for Experimental Biology.

1 | INTRODUCTION

Maternal obesity (MO) has become a significant public health concern globally with its prevalence rising exponentially.^{1,2} MO before and during pregnancy impacts offspring development,³ developmentally programming offspring for predisposition to obesity and associated cardiometabolic disorders including insulin resistance, heart disease, hypertension, and vascular dysfunction in later life.⁴ Many studies have attempted to identify the mechanisms that predispose to age-related, later-life metabolic diseases in offspring born to obese mothers, including the altered expression of genes involved in PPAR signaling, gluconeogenesis, lipid metabolism pathways, mitochondrial dysfunction, oxidative stress, and systemic inflammation.^{5,6} However, underlying molecular mechanisms still remain imperfectly understood and have not been examined comprehensively across multiple offspring tissues.

The application of various ‘-omics’ technologies such as metabolomics provides a new opportunity to reveal novel molecular mechanisms underlying how MO leads to offspring age-related metabolic diseases. The metabolome is defined as the complete set of low molecular weight metabolites, usually ranging from 50 to 1500 Da in a biological system.⁷ These metabolites, considered the downstream products of other biomolecules (such as genes, mRNAs, and proteins), actively interact with all levels of biomolecules, and thus play essential and crucial roles in the regulation of biological systems.⁸ Mass spectrometry (MS) often coupled with gas chromatography (GC) or liquid chromatography (LC) is considered as the technology of choice employed in untargeted metabolomics investigations due to its high sensitivity.⁹ While both GC and LC are complementary to each other in metabolomics analysis, GC offers superior chromatographic resolution and peak capacity, especially for volatile, polar metabolites, and fatty acid analysis. However, GC requires additional sample preparation steps such as metabolite derivatization which is not required for LC-based analyses.¹⁰ Studies using liquid chromatography-mass spectrometry (LCMS) have identified metabolic characteristics in offspring of obese mothers, including altered serum levels of histidine, tyrosine, 1, 5-anhydroglucitol, acylcarnitines, and various plasma ceramides.^{11,12} While some of these previous studies have attempted to explain the mechanisms underlying the impact of MO on the offspring metabolic health outcomes, these have only relied on biofluids such as plasma or serum which do not represent changes in individual tissues.

Studies of developmental programming including MO and the effect on the offspring have relied extensively on rodent models, with few studies performed in non-human primate (NHP) models in part because of their long

gestational period as well as the high cost of maintaining them.^{13,14} The baboon is a well-established NHP, a powerful translational model to understand the pathogenesis of cardiometabolic diseases in offspring born to obese mothers as they are a species closely related to humans. The baboon has been used as a model to study the genetics of various cardiometabolic disorders, including insulin resistance, obesity, heart disease, hypertension, and osteoporosis.¹⁵ These studies have significant translational value since baboons share strong genetic, metabolic, and physiological similarities with humans. For instance, lipid metabolism in baboons correlates strongly with humans and is more similar than other NHPs such as rhesus macaques, cynomolgus macaques, or vervet monkeys.¹⁶ Moreover, plasma cholesterol and triglyceride (TG) concentrations respond to dietary cholesterol, fat, and carbohydrates similar to humans.^{16,17}

In the present study, we sought to use an untargeted metabolomics approach to analyze liver and skeletal muscle biopsies as well as plasma samples from post-pubertal baboon MO offspring aged 3–6.5 years old (9–19.5 years old human equivalent) to identify early changes in metabolites and pathway perturbations in MO offspring prior to clear clinical onset of cardiometabolic abnormalities. Mothers of offspring were either fed a standard low cholesterol, low fat (chow) diet (CON)¹⁸ throughout life or a high energy diet, high-fat diet for at least 9 months before conception and during pregnancy and lactation (MO).¹⁴ All offspring consumed the standard control diet after weaning (Figure 1). The primary goals of this untargeted metabolite profiling in blood, liver, and skeletal muscle were to understand whether metabolic changes in adult offspring can be detected in tissues before they are detectable in circulation, and to determine whether changes that may eventually contribute to the development of metabolic diseases in offspring later in life are, common to, or different among, plasma, liver, and skeletal muscle. Moreover, we investigated whether metabolic changes in MO offspring were sex-specific since both normative aging and programmed changes in many age-related cardiometabolic diseases are often sexually dimorphic.

2 | MATERIALS AND METHODS

2.1 | Animal husbandry, protocol, and ethical clearance

All animal procedures were approved by the Texas Biomedical Research Institute's Institutional Animal Care and Use Committee (IACUC protocol number 1675 PC, September 30, 2018). Southwest National

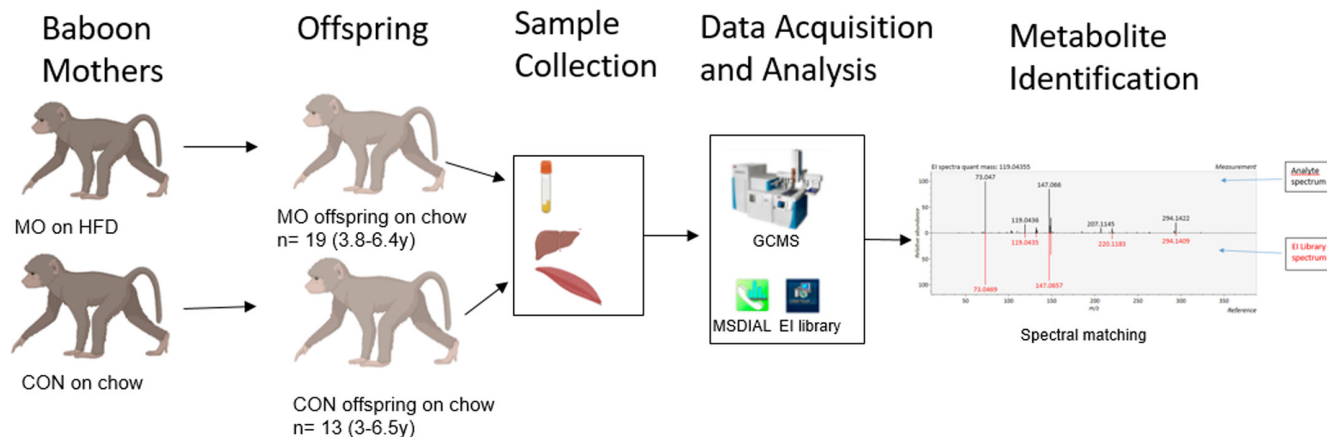


FIGURE 1 Study design and metabolomics workflow. Baboon mothers were fed a HFD or chow diet prior to and during pregnancy, and their offspring were weaned to a chow diet. Tissue and blood samples were collected from offspring animals once they reached early post-puberty for metabolomic data acquisition, metabolite identification, and quantification.

Primate Research Center (SNPRC) facilities at the Texas Biomedical Research Institute and the animal use programs and facilities are accredited by the Association for Assessment and Accreditation of Laboratory Animal Care International (AAALAC) which operates according to the National Institutes of Health (NIH) and U.S. Department of Agriculture guidelines. All animal care decisions were made by the SNPRC veterinarians, all of whom are AAALAC certified. All animals were housed in group cages allowing them to live in groups with normal social interactions and physical activity. All animals had ad libitum access to food and water. Enrichments, including toys, food treats, and music were provided on a daily basis by the SNPRC veterinary and behavioral staff in accordance with AAALAC, NIH, and U.S. Department of Agriculture guidelines.

2.2 | Study design and sample collection

Details of the study design have been described in detail elsewhere by Li et al.¹⁴ Briefly, female baboons were maintained in custom-built group cages with up to 16 females and a vasectomized male that allowed normal physical and social interaction and environmental enrichment at SNPRC. Females were randomly assigned prior to breeding to the CON or MO group. CON mothers ate SNPRC biscuits (Purina Monkey Diet and Monkey Diet Jumbo, Purina Lab Diets, St Louis, MO) which contained 12% energy fat, 0.29% glucose, 0.32% fructose, and a 3.07 kcal/g metabolizable energy ad libitum. For at least 9 months prior to breeding, MO mothers were fed ad libitum Purina 5045–6 (Purina Lab Diets, St Louis, MO, USA), a high fat and high energy diet (HFD) made up of 45% energy fat, 4.6% glucose, 5.6% fructose, and a

4.03 kcal/g metabolizable energy with equal access to the CON diet ad libitum. We have observed in many studies that mothers eat more of each diet when provided both. MO mothers also had continuous ad libitum access to a high fructose beverage and water.¹⁹ At the appropriate time, a proven breeder male was introduced into the cage. Following delivery, mothers were maintained on their pregnancy diet until offspring were weaned. At weaning, all offspring were weaned onto a chow diet¹⁸ at approximately 9 months of age. Following weaning, offspring were sorted into male and female juvenile groups and continued to feed ad libitum chow diet. At 3–6.5 years of age (9–19.5 years old human equivalent), liver and skeletal muscle biopsies, and plasma samples were collected. Freshly collected plasma samples were aliquoted and stored at -80°C until analysis. Tissue biopsies were immediately snap-frozen in liquid nitrogen upon collection and stored at -80°C until analysis. The distribution of offspring of CON and MO animals studied by age and sex is shown in Table 3.

2.3 | Sample processing

The extraction of metabolites from the liver, skeletal muscle, and plasma samples was performed following a protocol adopted from a previously described study by Misra et al.²⁰ In brief, aliquots (15 μl) of plasma or tissue homogenates were subjected to sequential solvent extraction, once each with 1 ml of acetonitrile: isopropanol: water (3:3:2) and 500 μl of acetonitrile: water (1:1) mixtures at 4°C .²¹ An internal standard, adonitol (2 μl from 10 mg/mL stock), was added to each aliquot prior to the extraction. Extracts were then dried under vacuum at 4°C prior to chemical derivatization (silylation

reactions). Blank tubes without samples, treated similarly to sample tubes, were included to account for any background noise and other sources of contamination. Samples and blanks were sequentially derivatized with methoxyamine hydrochloride (MeOX) and 1% TMCS in N-methyl-N-trimethylsilyl-trifluoroacetamide (MSTFA) or 1% TMCS containing N-(t-butyldimethylsilyl)-N-methyltrifluoroacetamide (MTBSTFA) as described in Misra et al.²⁰ This involved addition of 20 μ l of MeOX (20 mg mL⁻¹) in pyridine to the dry extracts and incubation at 55°C for 60 min followed by the addition of 80 μ l MTBSTFA and incubation at 60°C for 1 h.

2.4 | GC/MS data acquisition and pre-processing

Data were acquired using a high-resolution/accurate (HRAM) Orbitrap MS (Q-Orbitrap MS, Thermo Fisher) coupled to gas chromatography (GC). In all cases, 1 μ l of the derivatized sample was injected into the TRACE 1310 GC (Thermo Scientific, Austin, TX) in a splitless (SSL) mode at 220°C. The carrier gas was helium and the flow rate was 1 ml/min for separation on a Thermo Scientific Trace GOLD TG-5SIL-MS 30 m length \times 0.25 mm i.d. \times 0.25 μ m film thickness column with an initial oven temperature of 50°C for 0.5 min, followed by an initial gradient of 20°C/min ramp rate. The final temperature of 300°C was held for 10 min. Eluting peaks were transferred via an auxiliary transfer line into a Q Exactive-GC-MS (Thermo Scientific, Bremen, Germany). The total run time was 25 min. All data were acquired in a full scan electron ionization MS (EI MS1) mode at 70 eV energy, emission current of 50 μ A, and an ion source temperature of 250°C. A filament delay of 5.7 min was selected to prevent excess reagents from being ionized. High-resolution EI spectra were acquired using 60 000 resolution (fwhm at m/z 200) with a mass range of m/z 50–650. The transfer line was set to 230°C and the ion source 250°C. Data acquisition and instrument control were carried out using Xcalibur 4.3 and TraceFinder 4.1 software (Thermo Scientific). The capillary voltage was 3500 V with a scan rate of 1 scan/s. Finally, raw data (.raw files) obtained from data acquired by GCMS were converted to .mzML formats using ProteoWizard's msConvert tool prior to data preprocessing using open source software, MS-DIAL 4.6 (Riken, Japan, and Fiehn Lab, UC Davis, Davis, CA, USA). MS-DIAL 4.6 was used for raw peak extraction and data baseline filtering and calibration of baseline, peak alignment, deconvolution analysis, peak annotation, and integration of the peak height followed as described.²² Key parameters included a peak width of 20 scan, a minimum peak height of 10 000

amplitudes applied for peak detection, a sigma window value of 0.5, and an EI spectra cutoff of 50 000 amplitudes for deconvolution. For the annotation setting, the retention time tolerance was 0.5 min, the m/z tolerance was 0.5 Da, the EI similarity cutoff was 60%, and the annotation score cutoff was 60%. In the alignment parameters setting process, the retention time tolerance was 0.5 min, and the retention time factor was 0.5. Spectral library matching for metabolite identification was performed using an in-house and public library consisting of pool EI spectra from MassBank, GNPS, RIKEN, and MoNA. Data were further normalized by QC-based-loess normalization followed by \log_{10} transformation and missing values were imputed based on the random forest imputation method.

2.5 | Statistical analysis

Statistical processing of metabolomics datasets was performed using statistical software R (Version 3.5.1). This includes univariate, unsupervised multivariate method Principal Component Analysis (PCA), and supervised multivariate methods, Sparse Partial Least Squares Discriminant Analysis (sPLS-DA). All values were presented as the mean \pm SEM, and differences between groups were examined for statistical significance by computing a linear model. The normalized and \log_{10} -transformed metabolite intensities were modeled as the outcome and batch, sex, and biopsy age were adjusted for as covariates. We modeled MO status as a predictor and also included the interaction between sex and MO status. We also ran separate analyses stratified by sex to determine whether metabolites identified in our interaction analysis were male- or female-specific. Based on which metabolites demonstrated suggestive evidence in each of our analyses they were placed into three possible categories: male-specific, female-specific, or shared. Male-specific metabolites included any metabolites that met our significance criteria in the interaction analysis and the male-only analysis. Similarly, female-specific metabolites included any metabolites that met our significance criteria in both the interaction analysis and the female-only analysis. Shared metabolites included any metabolites that met our significance criteria in the joint analysis adjusting for sex as a covariate. Metabolites meeting an unadjusted p -value $<$.05 were considered suggestive evidence for downstream pathway analysis and metabolites meeting an FDR-adjusted p -value $<$.05 were considered statistically significant. Pathway analyses were conducted on the MetaboAnalyst website²³ (<https://www.metaboanalyst.ca/>).

3 | RESULTS

A total of 32 baboon MO offspring that were fed a normal diet after weaning to post-pubertal age, were included in the current study. The ages of the animals at biopsy and blood sample collection were similar between MO and CON groups (Table 1).

3.1 | Metabolomic profiles of young MO (3.8–6.4 years) and CON (3–6.5 years) adult offspring

To obtain global metabolite data for liver, plasma, and skeletal muscle samples, an untargeted metabolomics approach was carried out using a Q-Exactive GC-High-Resolution Orbitrap Mass Spectrometer (QEGC-HRMS). In our analysis, we identified and quantified 351, 316, and 423 metabolites in liver, skeletal muscle, and plasma, respectively. Multivariate statistical analysis identified differences between MO and CON offspring samples. An unsupervised PCA analysis showed some separation between MO and CON offspring samples in all three tissues (Figure S1A–C). The differences were more apparent in a supervised sPLS-DA analysis which is a special case of PLS-DA for data selection and classification in a one-step procedure was used since the algorithm is more effective in reducing the original high-dimensional data to a smaller number of relevant and important metabolites for robust and easy-to-interpret discriminant models.²⁴ The sPLSDA score plots showed less overlap between MO and CON offspring in the liver when compared to skeletal muscle and plasma, suggesting that sPLSDA was able to better discriminate between MO and CON offspring in the liver than in the other samples (Figure 2A–C). Moreover, while the error rates for all sample types were quite high, the error rates for the liver samples were lower than for skeletal muscle and plasma (Figure 2D–F).

3.2 | Metabolic dysregulation between MO and CON offspring group

To identify altered metabolites in liver, skeletal muscle, and plasma, we computed linear models both stratified by sex and jointly with sex-adjusted as a covariate. Across all analyses, we reported a total of 58 metabolites that demonstrated suggestive differences between groups in the liver (Table 2), and 46 metabolites with suggestive differences between groups in skeletal muscle (Table 3). There were no metabolites with suggestive differences in plasma samples. Only 7 metabolites from the liver analysis passed

TABLE 1 MO and CON offspring by age, mean age, sex, and size

| Group | Age (years) | Mean age | Sex | N |
|-------|-------------|----------|-----|----|
| CON | 3–6.5 | 4.85 | M | 7 |
| | | 5.40 | F | 6 |
| MO | 3.8–6.4 | 4.76 | M | 9 |
| | | 4.75 | F | 10 |

Abbreviations: M, Male; F, Female; N, Size.

the FDR < 0.05 (Table S1), and none passed FDR in skeletal muscle.

Among the 58 liver metabolites that were significantly different between MO and CON offspring, most were either carbohydrate- or amino acid-related metabolites. Forty-five differential liver metabolites were downregulated and 13 differential metabolites in the liver were upregulated in MO compared to CON offspring (Table 2). Similarly, in skeletal muscle, among the 46 altered metabolites between MO and CON offspring, 28 were downregulated and 18 upregulated (Table 3).

Comparing altered metabolites between the liver and skeletal muscle samples, regardless of categorization (male, female, or shared analysis), 8 metabolites were significantly different in both liver and skeletal muscle. These metabolites were L-serine, GABA, D-(+)-mannose, meso-tartaric acid, L-glutamine, serotonin, 3-aminoisobutyric acid, and myo-inositol.

3.3 | Assessing sex-specific differential metabolites in MO offspring

In addition to the joint analysis that identified metabolites with suggestive evidence of differences between CON and MO offspring across both sexes, we also tested for sex-specific effects. In the liver dataset, we observed 8 metabolites that were only different in males, which were all downregulated and 11 metabolites that were only different in females, of which 10 were upregulated. Only 2-Methylhippuric acid was downregulated in the liver of female MO offspring (Table 2). In a similar analysis with the skeletal muscle dataset, we observed 21 metabolites downregulated in males only and 18 metabolites upregulated in females only (Table 3). No sex-specific metabolite changes were observed in the plasma samples.

3.4 | Pathway enrichment analysis of the liver, skeletal muscle, and sex-specific differential metabolites

To further characterize the metabolic processes of the significantly different metabolites identified between

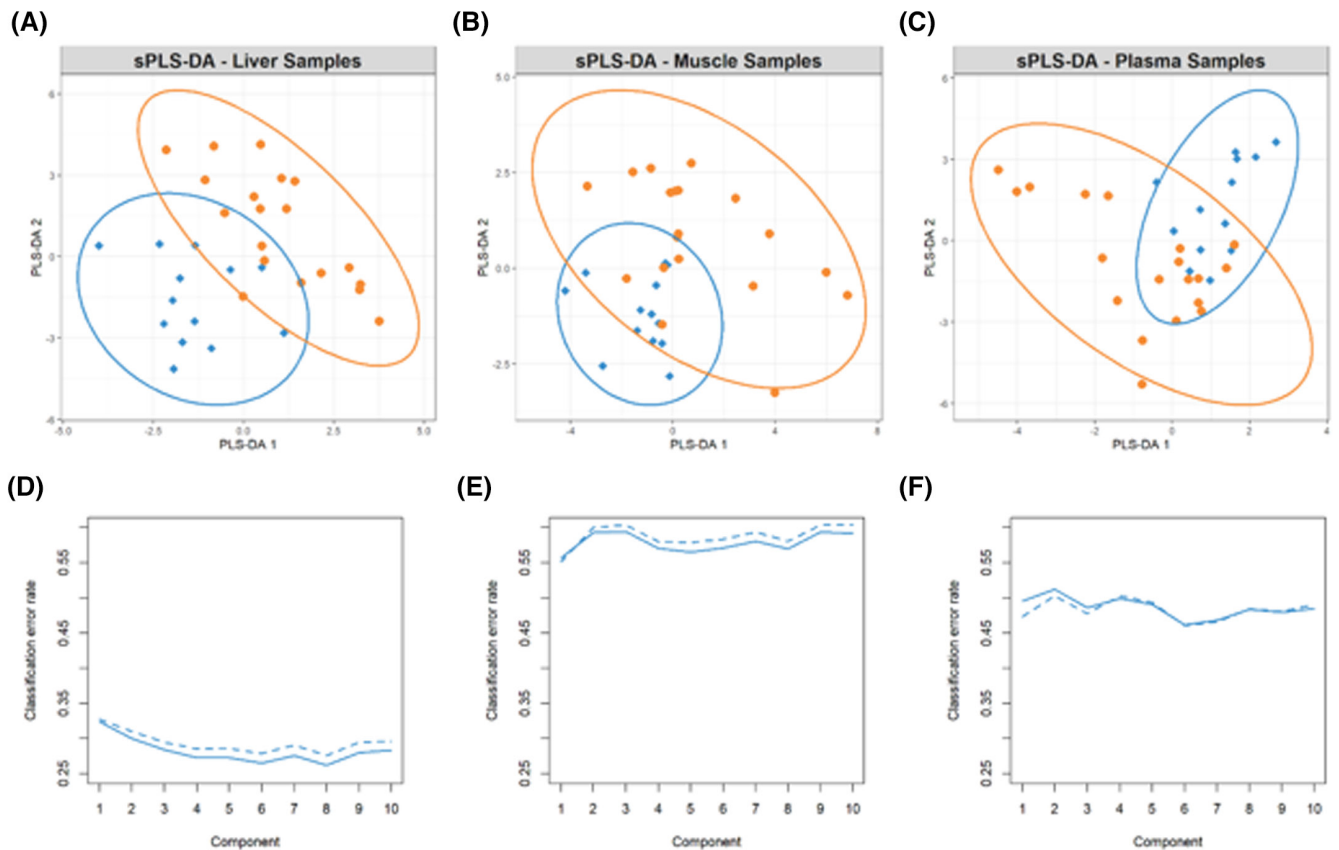


FIGURE 2 Sparse Partial Least Squares Discriminant Analysis (sPLS-DA) for all metabolites in liver, muscle, and plasma samples (MO: 3.8–6.4y, $n = 19$, 10 F and 9 M; CON: 3–6.5y, $n = 13$, 6 F and 7 M). (A, B and C) illustrate the maximum separation achieved between the control and MO samples in liver, muscle, and plasma samples, respectively. Controls are visualized as blue diamonds and MO samples are visualized as orange circles. 95% confidence intervals are illustrated as ellipses for each group of samples. None of the tissues demonstrate definite separation between the two groups. (D, E, and F) show the classification error rates computed for a mahalanobis distance between the two groups in liver, muscle, and plasma samples, respectively. The overall error rate is represented by a solid line and the balanced error rate is represented by a dashed line. The groups are well-balanced so a small difference between the overall error rate and the balanced error rate is expected.

MO and CON offspring, we used pathway enrichment analyses to map the liver and skeletal muscle differential metabolites using MetaboAnalyst 5.0 and KEGG library. This analysis revealed 9 metabolic pathways (Figure 3 and Table S2) that were significantly enriched using the 58 differential liver metabolites between MO and CON offspring. These metabolic pathways include arginine and proline metabolism, D-galactose metabolism, glutathione metabolism, nitrogen metabolism, and beta-alanine metabolism which were perturbed in MO offspring liver but not enriched in the skeletal muscle of the same offspring. In the skeletal muscle of MO offspring, using the 46 differential metabolites between MO and CON offspring, 10 metabolic pathways (Figure 4 and Table S3) were significantly enriched including citrate cycle (TCA cycle), butanoate metabolism, pantothenate and CoA metabolism, ascorbate and aldarate metabolism, cysteine, and methionine metabolism and glyoxylate and dicarboxylate metabolism. Moreover, pathways analyses showed that while

there were liver or skeletal muscle-specific altered metabolic pathways observed in MO offspring, 4 key pathways including alanine, aspartate, and glutamate metabolism, aminoacyl-tRNA biosynthesis, arginine metabolism, and D-Glutamine and D-glutamate metabolism were altered in both liver and skeletal muscle of MO offspring compared to CON offspring (Figures 3 and 4 and Table S4).

Pathway enrichment analysis for liver metabolites that differed only in males showed enrichment in arginine and proline metabolism. In contrast, female MO offspring showed enrichment of pathways related to tyrosine metabolism, nitrogen metabolism, and D-Glutamine and D-glutamate metabolism (data not shown). There was no overlap of altered skeletal muscle metabolic pathways between male and female MO offspring. While male MO skeletal muscle samples were enriched with pathways related to the TCA cycle, D-glutamine, and D-glutamate metabolism, alanine, aspartate and glutamate metabolism, pyridine metabolism, arginine biosynthesis, butanoate

TABLE 2 Summary of differential metabolites in the liver between MO (aged 3.8–6.4y, *n* = 19, 10 F and 9 M) and CON offspring (aged 3–6.5y, *n* = 13, 6 F and 7 M) listed with its respective group, category, log (FC), and *p*-value

| Metabolite | Group | Category | log(FC) | <i>p</i> -Value |
|---------------------------------------|-------------------------|----------|---------|------------------------|
| Fructose biphosphate | Sugar | Shared | −0.61 | 1.53×10^{-04} |
| Proline | Amino acid | Shared | −0.34 | 2.90×10^{-04} |
| 4-Methylumbelliferone | Hydroxycoumarin | Shared | −0.35 | 3.03×10^{-04} |
| Oxoproline | Amino acid | Shared | −0.33 | 3.74×10^{-04} |
| N-Acetylmannosamine | Acylaminosugar | Shared | −0.61 | 4.56×10^{-04} |
| Meso-tartarate | Sugar acid | Shared | −0.33 | 5.65×10^{-04} |
| Ribose-5-phosphate | Sugar conjugate | Shared | −0.44 | 9.19×10^{-04} |
| 4-Hydroxybenzoate | Benzoic acid | Shared | −1.07 | 1.16×10^{-03} |
| Maltose | Sugar | Shared | −0.37 | 2.48×10^{-03} |
| Galactose-6-phosphate | Sugar derivative | Shared | −0.37 | 2.48×10^{-03} |
| Asparagine | Amino acid | Shared | −0.36 | 5.20×10^{-03} |
| Spermidine | Amine | Shared | −0.39 | 6.19×10^{-03} |
| Adenosine | Purine nucleoside | Shared | 0.28 | 7.70×10^{-03} |
| 5-Sulfosalicylic acid | Benzenesulfonic acid | Shared | −0.12 | 8.45×10^{-03} |
| N-Methylaspartate | Amino acid | Shared | −0.43 | 1.02×10^{-02} |
| Glutamic acid | Amino acid | Shared | −0.43 | 1.02×10^{-02} |
| Sorbitol | Sugar conjugate | Shared | −0.33 | 1.33×10^{-02} |
| Serotonin | Tryptamine derivative | Shared | −0.52 | 1.33×10^{-02} |
| Azelate | Fatty acid | Shared | −0.22 | 1.71×10^{-02} |
| DL-Glyceraldehyde | Sugar | Shared | −0.85 | 1.78×10^{-02} |
| Myoinositol | Alcohol | Shared | −0.20 | 1.98×10^{-02} |
| Selenomethionine | Amino acid | Shared | −0.31 | 2.02×10^{-02} |
| Phosphate | Non-metal phosphate | Shared | −0.20 | 2.18×10^{-02} |
| 2,3-Diaminopropionate | Amino acid | Shared | −0.33 | 2.20×10^{-02} |
| 1,5-Anhydroglucitol | Sugar | Shared | −0.29 | 2.35×10^{-02} |
| Phosphoserine | Amino acid | Shared | −0.19 | 2.46×10^{-02} |
| DL-alpha, epsilon-Diaminopimelic acid | Amino acid | Shared | −0.15 | 2.59×10^{-02} |
| D-Arabinose 5-phosphate | Sugar conjugate | Shared | 0.21 | 2.65×10^{-02} |
| Resveratrol | Stilbene | Shared | −0.12 | 2.89×10^{-02} |
| alpha-Methylserine | Amino acid | Shared | −0.23 | 3.11×10^{-02} |
| Aspartic acid | Amino acid | Shared | −0.27 | 3.33×10^{-02} |
| alpha-D-Glucose | Sugar | Shared | −0.65 | 3.38×10^{-02} |
| 6-Carboxyhexanoate | Fatty acid conjugate | Shared | −0.17 | 3.54×10^{-02} |
| 1,6-Anhydro-beta-D-glucose | Sugar conjugate | Shared | −0.26 | 3.69×10^{-02} |
| Dithiothreitol | Dithiane | Shared | −0.12 | 3.88×10^{-02} |
| L-Serine | Amino acid | Shared | −0.27 | 4.70×10^{-02} |
| Cyclopentanone | Carbonyl compound | Shared | 0.31 | 4.94×10^{-02} |
| Lyxose | Sugar | Shared | −0.17 | 4.95×10^{-02} |
| DL-Cystathionine | Amino acid conjugate | Shared | −0.20 | 4.96×10^{-02} |
| 2-Methylhippuric acid | Benzoic acid derivative | Female | −1.04 | 1.80×10^{-03} |
| Methyl-4-aminobutyrate | Amino acid | Female | 1.50 | 6.85×10^{-03} |
| 3,4-Dihydroxymandelic acid | Benzenediol | Female | 0.07 | 7.67×10^{-03} |
| P-Octopamine | Benzenoids | Female | 0.12 | 1.22×10^{-02} |

(Continues)

TABLE 2 (Continued)

| Metabolite | Group | Category | log(FC) | p-Value |
|------------------------|-------------------------|----------|---------|------------------------|
| n-Butylamine | Amine | Female | 0.53 | 1.28×10^{-02} |
| 1,3-Diaminopropane | Amine | Female | 0.21 | 1.49×10^{-02} |
| 6-Aminohexanoic acid | Fatty acid | Female | 0.21 | 1.49×10^{-02} |
| 3-Aminoisobutyric acid | Amino acid | Female | 0.20 | 1.60×10^{-02} |
| Glutaric acid | Dicarboxylic acid | Female | 0.16 | 3.77×10^{-02} |
| L-Glutamine | Amino acid | Female | 0.14 | 4.00×10^{-02} |
| Tyramine | Amine | Female | 0.07 | 4.62×10^{-02} |
| Cadaverine | Amine | Male | -0.52 | 1.56×10^{-03} |
| Harmaline | Alkaloid | Male | -0.52 | 1.56×10^{-03} |
| D-(+)-Mannose | Sugar | Male | -0.51 | 2.48×10^{-03} |
| D-(+)-Galactose | Sugar | Male | -0.48 | 3.25×10^{-03} |
| GABA | Amino acid derivative | Male | -0.51 | 5.34×10^{-03} |
| Niacinamide | Pyridinecarboxylic acid | Male | -0.32 | 1.12×10^{-02} |
| N-Acetylputrescine | Carboximidic acid | Male | -0.65 | 2.86×10^{-02} |
| L-Glutathione | Amino acid derivative | Male | -1.31 | 4.61×10^{-02} |

metabolism, propanoate, and glyoxylate and dicarboxylate metabolism, female MO offspring showed no significantly enriched pathways.

4 | DISCUSSION

Multiple compelling epidemiological and experimental studies have shown that MO during pregnancy has lasting effects on the long-term health of the offspring, including obesity, hyperglycemia, diabetes, and hypertension, which are key features of metabolic syndrome.^{25,26} The concept that the nutritional status of the mother during pregnancy influences the long-term adult health of the offspring has been termed “developmental programming”.^{13,27} However, the underlying molecular mechanism(s) mediating the impact of MO on the development of age-related cardiometabolic disorders later in the life of the offspring remain poorly understood. The goal of this study was to identify tissue-specific and shared metabolic pathways that are altered in MO offspring despite the same nutrition after weaning as the CON offspring, which may contribute to the development of cardiometabolic abnormalities. To do so, we characterized tissue-specific differences in metabolites in MO and CON offspring by performing metabolomics analyses of plasma, liver, and skeletal muscle samples. MO and CON offspring were fed a normal chow diet after weaning thereby ensuring that life-course changes were induced during fetal development by maternal nutrition. Offspring were post-pubertal aged 3–6.5 years old for the CON offspring and 3.8–6.4 years old for the MO offspring at the time of tissue biopsy and blood

collection with no indication of cardiometabolic disease, allowing the discovery of metabolic perturbations prior to clinical disease.

Supervised SPLS-DA of metabolomics data showed a clear separation between MO and CON offspring, indicating metabolic alterations and dysregulation, particularly in the liver. Liver samples showed better classification rates compared to skeletal muscle and plasma, indicating that the greatest metabolic dysregulation induced by developmental programming was in the liver. The fact that MO and CON offspring were fed the same chow diet and lived in the same social groups emphasizes that differences between groups are very likely due to developmental programming effects mediated by differences in the maternal diet.

Univariate statistical analysis to investigate differential metabolites between MO and CON offspring revealed several altered metabolites with the liver (58 metabolites) showing a more altered metabolite profile in MO offspring than either skeletal muscle (46 metabolites) or plasma (0 metabolites). This observation was consistent in both the shared and sex-specific analyses. Similar differences in the liver compared to other tissues have been observed in postnatal dietary studies in mice. A previous LC-MS/MS metabolomics analysis of liver, serum, and intestine which compared mice fed a high-fat diet versus a control chow diet reported 47 altered metabolites in the liver, 7 in the serum, and 56 in the intestine with 17 metabolites shared between liver and small intestine.⁸ Interestingly, we see a similar magnitude of differences induced by maternal nutritional differences in utero that are maintained into the post-pubertal age

TABLE 3 Summary of differential metabolites in skeletal muscle between MO (aged 3.8–6.4 y, $n = 19$, 10 F and 9 M) and CON offspring (aged 3–6.5 y, $n = 13$, 6 F and 7 M) listed with its respective group, category, log (FC), and p -value

| Metabolite | Group | Category | log(FC) | p -Value |
|-----------------------------------|-------------------------------|----------|---------|------------------------|
| L-Serine | Amino acid | Shared | -0.89 | 2.17×10^{-02} |
| L-Gulcono-1,4-lactone | Sugar conjugate | Shared | -0.89 | 2.73×10^{-02} |
| Cysteine | Amino acid | Shared | -0.72 | 2.86×10^{-02} |
| GABA | Amino acid derivative | Shared | -0.77 | 3.89×10^{-02} |
| L-Valine | Amino acid | Shared | -0.72 | 4.06×10^{-02} |
| 3,4-Dihydroxyphenylglycol | Benzenediol | Shared | -0.76 | 4.27×10^{-02} |
| Norvaline | Amino acid | Shared | -0.72 | 4.44×10^{-02} |
| 3,6-Anhydro-d-hexose | Sugar | Female | 0.28 | 4.69×10^{-04} |
| Adipate | Organic acid | Female | 3.18 | 1.12×10^{-02} |
| Capric acid | Fatty acid | Female | 0.27 | 1.32×10^{-02} |
| D-(+)-Mannose | Sugar | Female | 0.49 | 1.32×10^{-02} |
| Lactose | Sugar | Female | 0.60 | 1.51×10^{-02} |
| Isothreonic acid | Sugar acid | Female | 0.44 | 1.75×10^{-02} |
| L-Gulonolactone | Lactone | Female | 2.12 | 1.86×10^{-02} |
| Salicylic acid | Benzoic acid | Female | 0.32 | 2.15×10^{-02} |
| 3-Hydroxybenzoate | Benzoic acid | Female | 0.32 | 2.15×10^{-02} |
| Homogentisate | Phenylacetic acid | Female | 2.06 | 2.25×10^{-02} |
| Mevalonate | Fatty acid | Female | 0.56 | 2.34×10^{-02} |
| Cerotinic acid | Fatty acid | Female | 0.67 | 2.76×10^{-02} |
| 3',5'-Cyclic AMP | Purine nucleotide | Female | 1.51 | 3.06×10^{-02} |
| Methionine | Amino acid | Female | 0.86 | 3.30×10^{-02} |
| 2'-Deoxyadenosine | Purine 2'-deoxyribonucleoside | Female | 0.22 | 4.41×10^{-02} |
| Meso-tartarate | Sugar acid | Female | 0.29 | 4.45×10^{-02} |
| Rhamnose | Sugar | Female | 0.58 | 4.54×10^{-02} |
| Hydroxybutyric acid | beta hydroxy acid | Female | 0.49 | 4.69×10^{-02} |
| Ibuprofen | Phenylpropanoic acid | Male | -0.55 | 1.12×10^{-02} |
| DL-Pipecolic acid | Amino acid | Male | -0.70 | 1.15×10^{-02} |
| 3-Pyridylacetic acid | Pyridine | Male | -0.77 | 1.30×10^{-02} |
| Succinic acid | dicarboxylic acid | Male | -0.49 | 1.57×10^{-02} |
| Aconitic acid | tricarboxylic acid | Male | -0.50 | 1.89×10^{-02} |
| beta-Alanine | Amino acid | Male | -0.70 | 2.47×10^{-02} |
| Inosine-5'-monophosphate | Purine ribonucleotide | Male | -0.50 | 2.57×10^{-02} |
| L-Glutamine | Amino acid | Male | -0.48 | 2.85×10^{-02} |
| Methylglutarate | Fatty acid | Male | -0.56 | 2.85×10^{-02} |
| DL-Threo-beta-methylaspartic acid | Amino acid derivative | Male | -0.53 | 2.97×10^{-02} |
| Cytidine monophosphate | Pyrimidine ribonucleotide | Male | -0.42 | 3.21×10^{-02} |
| Serotonin | Tryptamine derivative | Male | -0.31 | 3.74×10^{-02} |
| Maltotriose | Sugar | Male | -0.48 | 3.78×10^{-02} |
| 2-Oxoglutarate | gamma-keto acid derivative | Male | -0.54 | 3.84×10^{-02} |
| Meso-erythritol | Sugar conjugate | Male | -1.52 | 3.93×10^{-02} |
| 3-Aminoisobutyric acid | Amino acid | Male | -0.64 | 3.99×10^{-02} |
| Myoinositol | Alcohol | Male | -0.52 | 4.42×10^{-02} |
| Trehalose | Sugar | Male | -0.30 | 4.57×10^{-02} |
| Phosphoenolpyruvate | Alpha keto acid derivative | Male | -0.42 | 4.57×10^{-02} |
| DL-2,3-Diaminopropionic acid | Amino acid derivative | Male | -0.57 | 4.74×10^{-02} |
| 5-Aminovaleric acid | Delta amino acid derivative | Male | -0.44 | 4.99×10^{-02} |

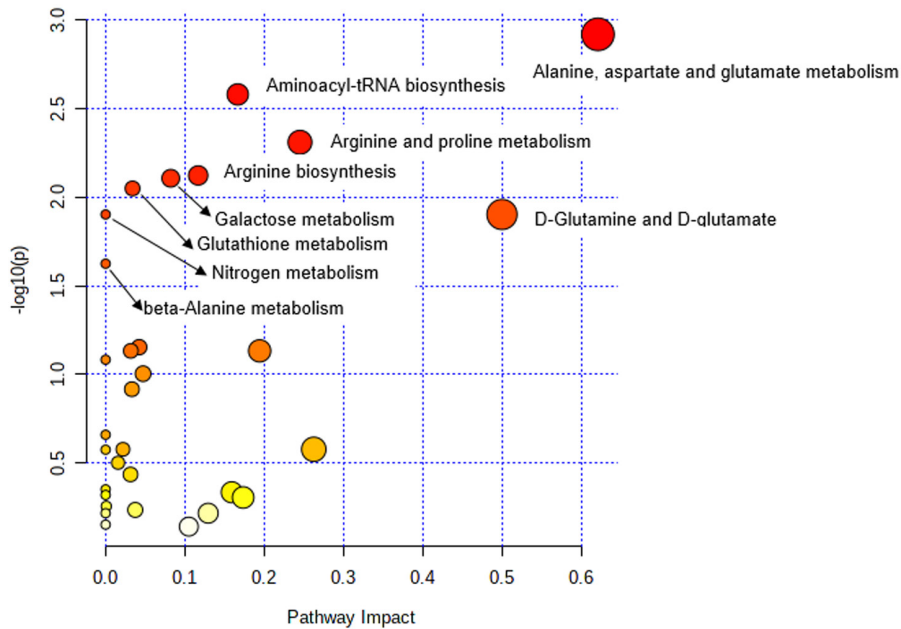


FIGURE 3 Pathway analysis for differential liver metabolites for MO (aged 3.8–6.4 y, $n = 19$, 10 F and 9 M) vs CON (aged 3–6.5 y, $n = 13$, 6 F and 7 M) offspring. Global metabolite pathways related to the perturbations of MO were performed using the online version of MetaboAnalyst based on all the differential metabolites listed in Table 2. All pathways were shown with p values reflecting the significance of pathway enrichment (y axis) and pathway impact values from pathway topology analysis (x axis), with the most impacted pathways colored in red. Pathways with significant p -value $< .05$ are annotated.

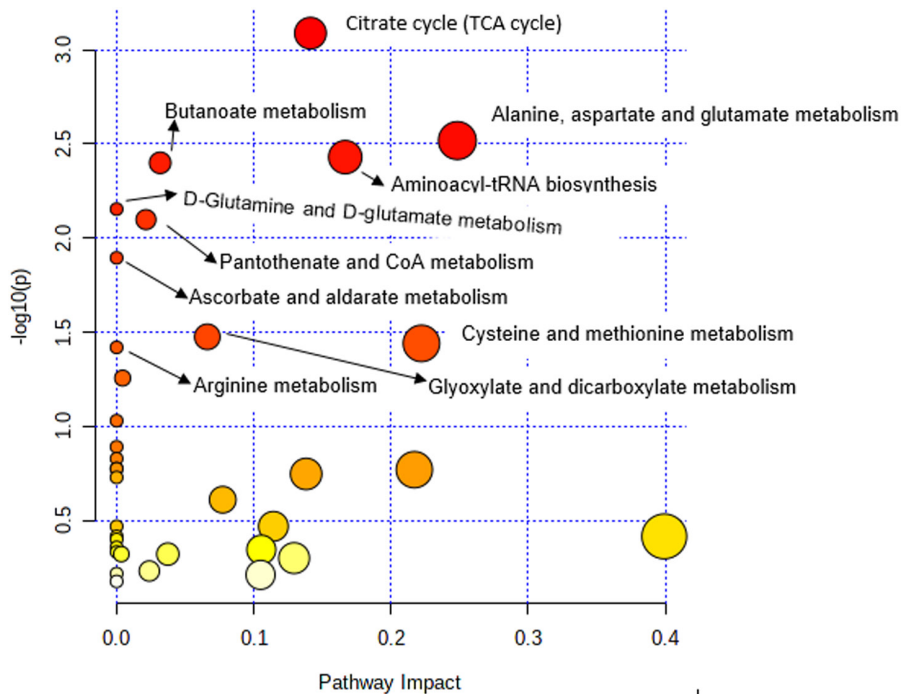


FIGURE 4 Pathway analysis for differential skeletal muscle metabolites for MO (aged 3.8–6.4 y, $n = 19$, 10 F and 9 M) vs CON (aged 3–6.5 y, $n = 13$, 6 F and 7 M) offspring. Global metabolite pathways related to the perturbations of MO were performed by the website of MetaboAnalyst based on all the differential metabolites listed in Table 3. All matched pathways were shown according to p values reflecting the significance of pathway enrichment analysis (y axis) and pathway impact values from pathway topology analysis (x axis), with the most impacted pathways colored in red. Pathways with significant p -value $< .05$ are annotated.

of the offspring despite the identical post-weaning nutrition of the animals. Interestingly, however, the changes seen in our study in liver and skeletal muscle are not reflected in the plasma, in contrast to the rodent studies of acute diet effects where plasma metabolites are also significantly changed. This suggests that there are early onset metabolic changes in tissues, particularly in the liver, which persist postnatally, and these changes are not reflected in circulatory metabolites. Moreover, the liver and skeletal muscle share several altered metabolites and altered metabolic pathways which is an

indication of the muscle-liver axis at the center of the metabolic derangement cascade as reported in rodent studies.²⁸ Our liver and skeletal muscle metabolomics analysis revealed lower abundances of dysregulated metabolites unique to male adult MO offspring and higher abundances of dysregulated metabolites specific to female MO offspring. This suggests that long-term metabolic changes in male MO offspring are different from female MO offspring. A previous multi-omics study in mice revealed sex-specific metabolic pathways. The authors reported that vitamin and cofactor metabolism

and ion channel transport were only altered in females, while phospholipid, lysophospholipid, and phosphatidylinositol metabolism and insulin signaling pathways were dysregulated in males in a liver disorder, NAFLD.²⁹ Moreover, the different metabolic regulation between males and females is consistent with the Li et al study where male MO offspring baboons increased in body weight at 2 years of weight assessment but no significant growth was observed in females within the same time point even though there was no body weight difference between control and MO offspring at the time of weaning for both sexes.¹⁴

Pathway analysis of differential metabolites suggests that carbohydrate metabolism and amino acid metabolism were the most significantly altered in both the liver and skeletal muscle of MO offspring. Since these two tissues are the main site for metabolism of glucose, fat, and amino acids, altered metabolism in these tissues may be an indication of metabolic impairment induced during development in utero by early exposure to poor maternal nutrition. In livers of MO offspring, we found significantly downregulated sugar metabolites (including fructose biphosphate, N-acetyl mannosamine, D-mannose, maltose, galactose-6-phosphate, D-galactose, DL-glyceraldehyde, 1, 5-anhydroglucitol, alpha-D-glucose, 1, 6-anhydro-beta-D-glucose, and lyxose), many involved in the galactose metabolism pathway. In skeletal muscle, altered sugar metabolites were either down-regulated (such as maltotriose and trehalose) or up-regulated (including D-mannose, lactose, rhamnose), and TCA cycle and glyoxylate and dicarboxylate metabolism pathways were altered in MO offspring. Altered galactose metabolism has been associated with disturbances in metabolic disorders of carbohydrates in the liver, and increased cholesterol concentration which predisposes to age-related diseases such as cardiovascular disease and non-alcoholic fatty liver disease.³⁰ A previous mouse study investigating the impact of maternal and post-weaning metabolic status on the adult male offspring's metabolome showed an alteration of carbohydrate-related pathways observed in MO offspring similar to our study.³¹ However, it is worth mentioning that MO offspring in the rodent study fed high-fat diets post-weaning, which differed from our study where MO offspring fed low cholesterol, low-fat chow diet (healthy control diet) post-weaning to early puberty. This means that there are possible metabolic imprinting effects caused by early maternal poor nutrition which persists irrespective of dietary changes after weaning and beyond, hence predisposing to age-related diseases.

Dysregulation of amino acid metabolism induced by MO has been reported in baboons¹⁹ which can predispose the offspring to several cardiometabolic diseases later in life.³² Using our sensitive untargeted metabolomics

method to investigate the impact of MO on post-natal offspring fed a healthy chow diet since weaning, we observed that several amino acid metabolites and pathways were dysregulated. This dysregulation was greatest in the liver, which is consistent with the liver serving as the primary site of protein and amino acid metabolism. Several liver amino acids including L-serine, glutamic acid, asparagine, proline, oxoproline, N-methylaspartate, selenomethionine, phosphoserine, alpha-methylserine, and DL-cystathione were all downregulated and L-Glutamine and 3-aminobutyric acid were upregulated in the MO offspring compared to CON offspring. Metabolic pathways related to amino acid metabolism altered in the liver included alanine, aspartate and glutamate metabolism, arginine and proline metabolism, arginine biosynthesis, glutathione metabolism, D-Glutamine and D-glutamate metabolism, and nitrogen metabolism. Analysis of the skeletal muscle metabolite dataset showed downregulation of several amino acid-related metabolites including L-serine, cysteine, GABA, L-valine, norvaline, beta-alanine, L-glutamine, 5-aminovaleric acid, and 3 of the amino acid metabolism-related pathways observed in MO offspring livers such as alanine, aspartate and glutamate metabolism, D-glutamine and D-glutamate metabolism, and arginine metabolism. In addition, MO offspring skeletal muscle showed dysregulation of cysteine and methionine metabolic pathways. Concentrations of methionine, glycine, serine, and taurine were lower in MO fetuses in a previous targeted study that focused on investigating the impact of MO on fetal methionine cycle biomarkers in baboons.¹⁹ These circulatory fetal metabolite changes did not persist in our post-natal MO offspring. However, amino acid metabolites and pathway alterations did persist in the liver and skeletal muscle as reported in our current study. We also observed alteration of the aminoacyl-tRNA biosynthesis pathway in both the liver and skeletal muscle of MO which is consistent with a previous study in mice fed HFD,⁸ further supporting the hypothesis that metabolic programming in utero has consequences similar to poor nutrition in postnatal animals. Our current findings suggest these pathways might be therapeutic targets for the prevention of the early onset of age-associated metabolic disorders in later life.

In summary, we used a well-established NHP baboon model of developmental programming by maternal diet and an untargeted metabolomics approach to show that MO leads to early tissue metabolic impairment, especially in the livers of MO offspring. The tissue-specific alterations in liver and skeletal muscle were not reflected in plasma. In addition, this study revealed sex- and tissue-specific altered metabolites in the MO offspring, with very little overlap across sample types. Further, our analysis identified key early metabolic pathways

specifically involved in carbohydrate and amino acid metabolism which were dysregulated in MO offspring in both liver and skeletal muscle, including alanine, aspartate and glutamate metabolism, aminoacyl-tRNA biosynthesis, arginine metabolism, and D-glutamine and D-glutamate metabolism. These pathways are implicated in many cardiometabolic diseases including NAFLD and CVD.³⁰ Therefore, this study provides initial global metabolic insights into the putative long-term implications of MO on offspring in predisposing them to metabolic disorders in later life. Further studies are needed to investigate the metabolic changes in tissues and plasma altered as these animals age, and whether they develop cardiometabolic abnormalities at younger ages than the CON animals. That is, do these early-life metabolic disturbances predict long-term health? Once validated, these early metabolic changes in the liver may serve as targets to develop effective treatments for age-related metabolic disorders that are likely to develop in adulthood due to developmental MO exposure.

AUTHOR CONTRIBUTIONS

Ge Li collected initial samples, and prepared sample aliquots for metabolomics experiments; Isaac Ampong processed the samples, acquired and processed the metabolomics dataset, and wrote the manuscript; Katharyn E. Wallis and Danu S. Perumalla assisted in sample processing; Isaac Ampong and Kip D. Zimmerman performed the identification/annotation of metabolites, metabolic pathway, and statistical analysis; Isaac Ampong, Kip D. Zimmerman and Michael Olivier interpreted the results; Kip D. Zimmerman, Peter W. Nathanielsz, Laura A. Cox, and Michael Olivier reviewed the initial manuscript draft; Hillary F. Huber and Cun Li were involved in animal management and maintenance; Peter W. Nathanielsz, Laura A. Cox, and Michael Olivier provided materials, funding, and resources; and all authors revised the final manuscript draft and agreed to the published version of the manuscript.

ACKNOWLEDGMENTS

This work was funded by the National Institute of Health (NIH) grant U19 AG057758 to PWN, LAC, and MO. The authors would like to also acknowledge the Texas Biomedical Research Institute staff for the veterinary services and animal maintenance support.

DISCLOSURES

The authors declare no competing interests.

DATA AVAILABILITY STATEMENT

All mass spectral spectra data generated in this study are deposited at the metabolomics workbench with Study

ID ST002254 (DatatrackID:3379) and available at this link <http://dev.metabolomicsworkbench.org:22222/data/DRCCMetadata.php?Mode=Study&StudyID=ST002254&Access=RcoK5835> [dev.metabolomicsworkbench.org] Spectral libraries are available on request from the corresponding author.

ORCID

Michael Olivier  <https://orcid.org/0000-0003-1632-1063>

REFERENCES

1. Long NM, Rule DC, Tuersunjiang N, Nathanielsz PW, Ford SP. Maternal obesity in sheep increases fatty acid synthesis, upregulates nutrient transporters, and increases adiposity in adult male offspring after a feeding challenge. *PLoS One*. 2015;10(4):e0122152.
2. Chen C, Xu X, Yan Y. Estimated global overweight and obesity burden in pregnant women based on panel data model. *PLoS One*. 2018;13(8):e0202183.
3. Nelson SM, Matthews P, Poston L. Maternal metabolism and obesity: modifiable determinants of pregnancy outcome. *Hum Reprod Update*. 2010;16(3):255-275.
4. Wang Q, Zhu C, Sun M, et al. Maternal obesity impairs fetal cardiomyocyte contractile function in sheep. *FASEB J*. 2019;33(2):2587-2598.
5. Alfaradhi MZ, Fernandez-Twinn DS, Martin-Gronert MS, Musial B, Fowden A, Ozanne SE. Oxidative stress and altered lipid homeostasis in the programming of offspring fatty liver by maternal obesity. *Am J Physiol Regul Integr Comp Physiol*. 2014;307(1):R26-R34.
6. Lynch C, Chan CS, Drake AJ. Early life programming and the risk of non-alcoholic fatty liver disease. *J Dev Orig Health Dis*. 2017;8(3):263-272.
7. Viant MR, Kurland IJ, Jones MR, Dunn WB. How close are we to complete annotation of metabolomes? *Curr Opin Chem Biol*. 2017;36:64-69.
8. Zhu N, Huang S, Zhang Q, et al. Metabolomic study of high-fat diet-induced obese (DIO) and DIO plus CCl₄-induced NASH mice and the effect of obeticholic acid. *Metabolites*. 2021;11(6):374.
9. Ashrafian H, Sounderajah V, Glen R, et al. Metabolomics: the stethoscope for the twenty-first century. *Med Princ Pract*. 2021;30(4):301-310.
10. Ampong I, Zimmerman KD, Nathanielsz PW, Cox LA, Olivier M. Optimization of imputation strategies for high-resolution gas chromatography-mass spectrometry (HR GC-MS) metabolomics data. *Metabolites*. 2022;12(5):429.
11. León-Aguilar LF, Croyal M, Ferchaud-Roucher V, et al. Maternal obesity leads to long-term altered levels of plasma ceramides in the offspring as revealed by a longitudinal lipidomic study in children. *Int J Obes (Lond)*. 2019;43(6):1231-1243.
12. Snow SJ, Broniowska K, Karoly ED, et al. Offspring susceptibility to metabolic alterations due to maternal high-fat diet and the impact of inhaled ozone used as a stressor. *Sci Rep*. 2020;10(1):16353.
13. Schoonejans JM, Ozanne SE. Developmental programming by maternal obesity: lessons from animal models. *Diabet Med*. 2021;38(12):e14694.

14. Li C, Jenkins S, Considine MM, et al. Effect of maternal obesity on fetal and postnatal baboon (*Papio* species) early life phenotype. *J Med Primatol*. 2019;48(2):90-98.
15. Cox LA, Comuzzie AG, Havill LM, et al. Baboons as a model to study genetics and epigenetics of human disease. *ILAR J*. 2013;54(2):106-121.
16. Cox LA, Olivier M, Spradling-Reeves K, Karere GM, Comuzzie AG, VandeBerg JL. Nonhuman primates and translational research-cardiovascular disease. *ILAR J*. 2017;58(2):235-250.
17. Higgins PB, Bastarrachea RA, Lopez-Alvarenga JC, et al. Eight week exposure to a high sugar high fat diet results in adiposity gain and alterations in metabolic biomarkers in baboons (*Papio hamadryas* sp.). *Cardiovasc Diabetol*. 2010;9:71.
18. Mahaney MC, Karere GM, Rainwater DL, et al. Diet-induced early-stage atherosclerosis in baboons: lipoproteins, atherogenesis, and arterial compliance. *J Med Primatol*. 2018;47(1):3-17.
19. Nathanielsz PW, Yan J, Green R, et al. Maternal obesity disrupts the methionine cycle in baboon pregnancy. *Physiol Rep*. 2015;3(11):e12564.
20. Misra BB, Puppala SR, Comuzzie AG, et al. Analysis of serum changes in response to a high fat high cholesterol diet challenge reveals metabolic biomarkers of atherosclerosis. *PLoS One*. 2019;14(4):e0214487.
21. Fiehn O, Wohlgemuth G, Scholz M, et al. Quality control for plant metabolomics: reporting MSI-compliant studies. *Plant J*. 2008;53(4):691-704.
22. Tsugawa H, Cajka T, Kind T, et al. MS-DIAL: data-independent MS/MS deconvolution for comprehensive metabolome analysis. *Nat Methods*. 2015;12(6):523-526.
23. Chong J, Wishart DS, Xia J. Using MetaboAnalyst 4.0 for comprehensive and integrative metabolomics data analysis. *Curr Protoc Bioinformatics*. 2019;68(1):e86.
24. Lê Cao KA, Boitard S, Besse P. Sparse PLS discriminant analysis: biologically relevant feature selection and graphical displays for multiclass problems. *BMC Bioinformatics*. 2011;12:253.
25. Li M, Sloboda DM, Vickers MH. Maternal obesity and developmental programming of metabolic disorders in offspring: evidence from animal models. *Exp Diabetes Res*. 2011; 2011:592408.
26. Glasstras SJ, Chen H, Pollock CA, Saad S. Maternal obesity increases the risk of metabolic disease and impacts renal health in offspring. *Biosci Rep*. 2018;38(2):BSR2010050.
27. McCoski S, Bradbery A, Marques RDS, Posbergh C, Sanford C. Maternal nutrition and developmental programming of male progeny. *Animals (Basel)*. 2021;11(8):2216.
28. Romijn JA, Pijl H. The muscle-liver axis: does aerobic fitness induce intrahepatic protection against non-alcoholic fatty liver disease? *J Physiol*. 2009;587(Pt 8):1637.
29. Kurt Z, Barrere-Cain R, LaGuardia J, et al. Tissue-specific pathways and networks underlying sexual dimorphism in non-alcoholic fatty liver disease. *Biol Sex Differ*. 2018;9(1):46.
30. Zhou YY, Ji XF, Fu JP, et al. Gene transcriptional and metabolic profile changes in mimetic aging mice induced by D-galactose. *PLoS One*. 2015;10(7):e0132088.
31. Safi-Stibler S, Thévenot EA, Jouneau L, et al. Differential effects of post-weaning diet and maternal obesity on mouse liver and brain metabolomes. *Nutrients*. 2020;12(6):1572.
32. Jin R, Banton S, Tran VT, et al. Amino acid metabolism is altered in adolescents with nonalcoholic fatty liver disease—an untargeted, high resolution metabolomics study. *J Pediatr*. 2016;172:14-19.e5.

SUPPORTING INFORMATION

Additional supporting information can be found online in the Supporting Information section at the end of this article.

How to cite this article: Ampong I, Zimmerman KD, Perumalla DS, et al. Maternal obesity alters offspring liver and skeletal muscle metabolism in early post-puberty despite maintaining a normal post-weaning dietary lifestyle. *The FASEB Journal*. 2022;36:e22644. doi: [10.1096/fj.202201473R](https://doi.org/10.1096/fj.202201473R)